

# Paramagnetic Effect of Oxygen in the $^{23}\text{Na}$ MAS NMR and $^{23}\text{Na}$ MQMAS NMR Spectroscopy of Zeolite LiNaX

Robyn J. Accardi and Raul F. Lobo\*

Center for Catalytic Science and Technology, Department of Chemical Engineering, University of Delaware, Newark, Delaware 19716

Martin Kalwei

Institute for Physical Chemistry, University of Münster, Münster, Germany 48149

Received: November 17, 2000; In Final Form: February 28, 2001

The paramagnetic effects of oxygen molecules on the sodium cations in zeolite LiNaX ( $\approx 70\%$  Li;  $30\%$  Na) were investigated using variable-temperature  $^{23}\text{Na}$  MAS NMR and  $^{23}\text{Na}$  MQMAS NMR. The presence of the oxygen caused a downfield paramagnetic shift for the site III resonance, indicating the accessibility of these cation sites. Although a shift was realized, it is much smaller than what is observed for  $^7\text{Li}$  by others. To understand these results,  $^{23}\text{Na}$  MQMAS NMR was used to calculate the isotropic chemical shifts, quadrupolar shifts, and the quadrupolar coupling constants. The quadrupolar coupling constant and quadrupolar shift of the site III sodium remain the same irrespective of the presence or absence of oxygen; however, these values were affected by temperature changes and were found to increase at lower temperatures.

## Introduction

The appearance of magic angle spinning (MAS) nuclear magnetic resonance (NMR) spectra of extraframework cations in zeolites can be highly affected by the presence of a paramagnetic gas species in the sample.<sup>1–5</sup> The NMR peaks of nuclei in close contact with a paramagnetic species experience line broadening, shorter relaxation times, and paramagnetic shifts due to the interactions of the unpaired electron spin with the nuclear spin.<sup>6</sup> Comparisons have been made between the MAS NMR spectra of zeolites under vacuum and those containing physisorbed paramagnetic species,<sup>1–5</sup> and in the case of zeolites, if a cation site is in contact with a physisorbed paramagnetic species, the peak corresponding to that cation site will be shifted from its original position in the vacuum MAS NMR spectrum (i.e., the so-called paramagnetic shift). Resonances corresponding to cation sites that are not in close contact with the paramagnetic species will not observe a shift. The paramagnetic shift effect is inversely proportional to temperature ( $\Delta\nu \propto 1/T$ ) and thus as the temperature is decreased the paramagnetic shift will increase.<sup>6</sup>

We have used lithium NMR and the paramagnetic shift effect to study cation accessibility in zeolites beta and ZSM-5.<sup>7</sup> To date no one has studied the effect of a paramagnetic species on sodium cations in zeolites, and it is unknown if  $^{23}\text{Na}$  MAS NMR will provide as much information as its lithium counterpart.

Because of its high quadrupolar moment ( $1 \times 10^{-29}$  Q/m<sup>2</sup>),  $^{23}\text{Na}$  NMR spectra are not always easy to interpret. The interaction between the nuclear quadrupolar moment with the electric field gradient (EFG) at the nuclear site may give rise to complex, broad, and overlapping resonances.<sup>8</sup> The chemical shift of these resonances is affected not only by the local chemical environment around the nuclei but also by second-order upfield quadrupolar shifts.<sup>9</sup> These quadrupolar shifts are

inversely proportional to the magnetic field strength and thus spectrometers with high fields are desirable. Despite the difficulties in interpreting sodium NMR data, once analyzed correctly, NMR spectra of the quadrupolar nuclei can give information about the local electronic structure and geometry. Values for the isotropic chemical shifts, quadrupolar coupling constants, and second-order quadrupolar shifts can be determined using advanced NMR techniques.

To understand the interactions in quadrupolar nuclei, researchers have turned to two-dimensional multiquantum MAS NMR (2D MQMAS NMR).<sup>10–14</sup> Using this technique, shielding, quadrupolar, and dipolar anisotropies can be eliminated. The multiquantum technique diminishes the quadrupolar anisotropies by refocusing the second-order quadrupolar effects while the MAS averages out the shielding and dipolar anisotropies. This leads to increased spectral resolution.

In this paper we examine the effects of the adsorption of a paramagnetic species (dioxygen) on the sodium cations in site III of LiNaX (Figure 1) using variable-temperature  $^{23}\text{Na}$  MAS NMR and  $^{23}\text{Na}$  MQMAS NMR. LiNaX was used in this investigation for several reasons. LiNaX with sodium occupying site III will produce a simple sodium spectrum with one relatively sharp peak. In addition, it has been found that the lithium site III cations are accessible to oxygen molecules,<sup>1</sup> and therefore the site III sodium should also be accessible. The room-temperature  $^{23}\text{Na}$  MAS NMR spectrum of the oxygen-containing sample shows a downfield paramagnetic shift of the site III cation resonance from its position in the vacuum spectra (2.4 ppm). This shift indicates the accessibility of these sodium cations to the oxygen molecules. Although a paramagnetic shift is observed at low temperatures, this shift was much smaller than expected. The MQMAS spectra show that the quadrupolar coupling constants and the quadrupolar shifts of the room-temperature sodium resonance remain the same irrespective of the presence or absence of oxygen. Therefore, a significant

\* Corresponding author. E-mail: lobo@che.Udel.edu.

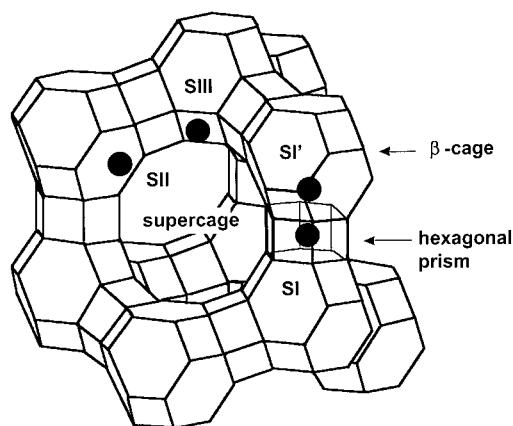


**Figure 1.** Site positions in zeolite X.

paramagnetic shift will be observed in the room-temperature NMR spectrum for the oxygen-containing sample. However, the upfield quadrupolar shift increases at lower temperatures such that a smaller downfield paramagnetic shift will be observed for the site III resonance in the low-temperature  $^{23}\text{Na}$  MAS NMR spectra.

### Experimental Section

**Sample Preparation.** A sample of approximately 10 g of NaX ( $\text{Si}/\text{Al} = 1$ ) was prepared using a synthesis gel with a stoichiometry<sup>15</sup> of  $\text{SiO}_2$ :  $\text{Al}_2\text{O}_3$ :  $5\text{NaOH}$ :  $1.5\text{ KOH}$ :  $55.25\text{ H}_2\text{O}$ .

NaX was prepared by ion-exchanging NaX with a 2 M NaCl solution containing 11.70 g of NaCl (Aldrich, 99+%) and 100 mL of deionized water, and the sample was exchanged at 100 °C for over 12 h. The sample was then filtered and washed with deionized water.

LiNaX with sodium in site III was made by starting with NaX. The sample was prepared by first exchanging NaX into the lithium form ( $\text{LiX}$ )<sup>2</sup>. We have found that samples of LiNaX can be prepared by quantitative exchanges of lithium for sodium starting with  $\text{LiX}$ .<sup>15</sup>

The dehydrated and oxygen-containing samples were prepared in 4 mm MAS NMR glass inserts (Wilma Glass). Complete dehydration was obtained by evacuating the samples below  $P = 10^{-1}$  Pa while heating at 1 °C/min to 120 °C. The sample was kept at this temperature for 8 h. The samples were then heated 2 °C/min to 400 °C and held at this temperature for 13 h. The dehydrated samples (under vacuum) were then sealed. The oxygen-containing samples were first dehydrated as described above. Before sealing, the samples were contacted with extra dry oxygen (Matheson, 99.6%) at a pressure of approximately 585 Torr.  $^1\text{H}$  MAS NMR was used to confirm that no water remained in the samples.

**Analytical Details.** X-ray powder diffraction patterns were obtained using a Philips X'pert system with  $\text{Cu K}\alpha$  radiation ( $\lambda = 1.54186 \text{ \AA}$ ). Nitrogen adsorption isotherms were obtained at 77 K using a Micromeritics ASAP 2010 adsorption machine. The samples were evacuated at 320 °C prior to the adsorption studies. The micropore volume was estimated by using the amount of nitrogen adsorbed per gram of zeolite ( $\text{cm}^3/\text{g}$ ) at a relative pressure  $P/P_0$  of 0.1. The density of liquid nitrogen was taken as 0.029 mol/mL. Chemical analysis was performed by Galbraith Laboratories, Inc. (Knoxville, TN.).

$^1\text{H}$ ,  $^{23}\text{Na}$ ,  $^{27}\text{Al}$ , and  $^{29}\text{Si}$  MAS NMR spectra were recorded using a Bruker MSL 300 MHz spectrometer operating at resonance frequencies of 300.13, 79.39, 78.205, and 59.627 MHz, respectively. The samples were spun in zirconia rotors. The  $^{27}\text{Al}$  MAS NMR spectra were obtained in a 4 mm probe

using a  $\pi/12$  pulse of  $1 \mu\text{s}$  and a recycle delay of 2 s. The samples were spun at 9 kHz, and the chemical shifts were referenced to a 1 M  $\text{Al}(\text{NO}_3)_3$  solution. The  $^{29}\text{Si}$  MAS NMR spectra were obtained in 7 mm rotors at a spinning rate of 3 kHz. 3-(Trimethylsilyl)-1-propanesulfonic acid (DSS) was used as the chemical shift reference. A  $\pi/3$  pulse of  $4 \mu\text{s}$  was used with a recycle delay of 15 s between each scan.  $^{23}\text{Na}$  NMR was used to check the completeness of the lithium ion exchange used to prepare LiX. The hydrated LiX sample was spun at 6 kHz in a 4 mm probe. The spectrum was obtained using a  $\pi/4$  pulse of  $2 \mu\text{s}$  and a recycle delay of 1 s. The spectrum was referenced to solid NaCl.  $^1\text{H}$  MAS NMR experiments were obtained in 4 mm rotors spinning at a rate of 6 kHz and the samples were referenced to Adamantane. A  $3.25 \mu\text{s}$   $\pi/2$  pulse was employed with a recycle delay of 15 s.

All other  $^{23}\text{Na}$  MAS NMR and  $^{23}\text{Na}$  MQMAS NMR were performed on a Bruker Avance DSX 500 MHz spectrometer operating at a frequency of 132.29 MHz. The  $^{23}\text{Na}$  MAS NMR spectra were obtained using a 4 mm triple resonance probe spinning at a rate of 10 kHz. The chemical shift was set using solid NaCl. A pulse length of less than  $\pi/8$  ( $3 \mu\text{s}$ ) was used with a recycle delay of 0.5 s. A total of 858 scans were taken for the LiNaX samples. Variable-temperature MAS NMR spectra were recorded by spinning the oxygen containing samples in nitrogen gas at temperatures of 260, 250, and 230 K. The temperatures were monitored using a Bruker variable-temperature unit.

$^{23}\text{Na}$  MQMAS NMR spectra were obtained using a three-pulse sequence with z-filtering. Variable-temperature  $^{23}\text{Na}$  MQMAS NMR spectra were recorded by spinning the oxygen-containing samples in nitrogen gas at a temperature of 250 K.

The MQMAS data were analyzed by performing a 2D Fourier transform with a shearing transformation to get a 2D spectrum with an isotropic frequency component along the F1 spectral axis and an anisotropic frequency along the F2 axis.<sup>16</sup> The isotropic chemical shifts, second-order quadrupolar shifts, and quadrupolar coupling constants were calculated.<sup>12–14</sup>

### Results

**Sample Characterization.** The X-ray powder diffraction patterns for all of the samples showed no amorphous backgrounds and no indication of impurities. The micropore volume determined from  $\text{N}_2$  adsorption isotherms was  $0.32 \text{ cm}^3/\text{g}$  for LiNaX, similar to that found in the literature for a similar sample.<sup>17</sup> From chemical analysis the Na/Al ratio and Li/Al ratio for LiNaX were found to be 0.327 and 0.652, respectively. Thus, approximately one-third of all cations in X are sodium cations. The  $^{27}\text{Al}$  MAS NMR spectra of LiNaX showed only one signal at approximately 54 ppm, which is assigned to tetrahedrally coordinated aluminum.<sup>18</sup> The  $^{29}\text{Si}$  MAS NMR spectra for LiNaX contained only one peak at approximately  $-84 \text{ ppm}$ , which corresponds to a silicon site surrounded by four aluminum atoms, thus indicating a Si/Al ratio of 1. This value is close to the Si/Al ratio calculated by chemical analysis, which was 1.03 for LiNaX.  $^{23}\text{Na}$  MAS NMR spectrum of the LiNaX sample indicates that the sodium was located mainly in site III, but a small fraction of the cations may be located in other sites.<sup>15</sup>

**$^{23}\text{Na}$  MAS NMR ( $B = 500 \text{ MHz}$ ).** The  $^{23}\text{Na}$  MAS NMR spectrum of LiNaX under vacuum is shown in Figure 2a (the signal from the glass insert has been subtracted from all of the  $^{23}\text{Na}$  MAS NMR spectra in this figure). LiNaX with varying sodium contents can produce  $^{23}\text{Na}$  MAS NMR spectra with up to six resonances corresponding to sodium located at sites SI, SI', SII, and three different SIII positions.<sup>19</sup> Figure 2a shows a

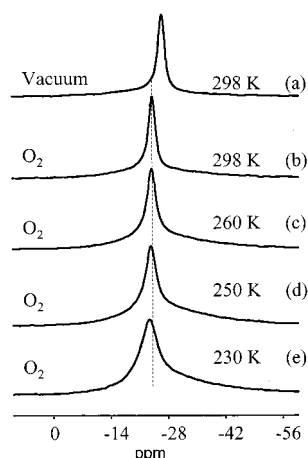


**Figure 2.**  $^{23}\text{Na}$  MAS NMR for LiNaX; (a) dehydrated (vacuum) room-temperature spectra; oxygen adsorbed spectra at (b) room temperature, (c) 260 K, (d) 250 K, and (e) 230 K.

sharp resonance at  $-26.6$  ppm, which has been assigned to the cations located at one of the SIII positions. Shoulders are observed on both the high- and low-frequency sides of the peak. The remainder of this paper will focus only on the sharp site III resonance.

Feuerstein et al. showed that as the composition of LiNaX approaches a content of 70% lithium and 30% sodium, the  $^{23}\text{Na}$  MAS NMR spectrum contains a single sharp resonance at approximately  $-30$  ppm ( $B = 400$  MHz).<sup>15</sup> The samples in their research were not under vacuum but instead were packed in a glovebox under dry nitrogen gas. The spectrum of the sample used in our studies shows this sharp peak at  $-26.6$  ppm. The difference in the location of the site III resonance is probably due to the difference in the magnetic fields. A higher field (500 MHz vs 400 MHz) will decrease the second-order quadrupolar shift so that the site III resonance will be shifted downfield.<sup>14</sup> The difference in chemical shift may be also due to the different sample environments and perhaps due to small differences in chemical composition.

The room-temperature spectrum of the oxygen-containing sample is shown in Figure 2b. The site III resonance is shifted downfield from  $-26.6$  to  $-24.2$  ppm, which is due to the paramagnetic effect of oxygen and indicates that sodium cations associated with this resonance are accessible to the oxygen molecules (as expected). We believe that this downfield shift is due to the paramagnetic effects of oxygen and is not caused by any nonparamagnetic interactions arising from the presence of an adsorbed species. Similar  $^{23}\text{Na}$  NMR experiments investigating the site III cations in NaX were performed, and samples under vacuum and in the presence of nitrogen were compared. The presence of the diamagnetic nitrogen caused only a very small upfield chemical shift of the sodium site III resonance from its position in the spectrum of the vacuum sample. Consequently, the substantial downfield shift seen in Figure 2b is due, for the most part, to paramagnetic effects.

Low-temperature  $^{23}\text{Na}$  MAS NMR spectra were recorded on the oxygen-containing sample (Figure 2c–e). As the temperature was lowered from 298 to 260 K the site III resonance is shifted slightly downfield to  $-24.1$  ppm. A further drop in the temperature to 250 K causes the peak to shift to  $-23.9$  ppm, and a drop to 230 K shifts the peak to  $-23.5$  ppm. This shift is smaller than what was expected from previous observations<sup>1,3</sup> and suggests that other effects (i.e., quadrupolar interactions, etc.) affect the spectra at lower temperatures.

Figure 2b–e also shows that the sodium peaks become broader after the adsorption of oxygen, especially at low

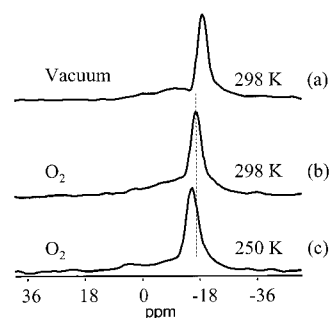


**Figure 3.**  $^{23}\text{Na}$  MQMAS NMR F1 dimension of LiNaX: (a) dehydrated (vacuum) room temperature; oxygen adsorbed spectra at (b) room temperature and (c) 250 K.

**TABLE 1:  $^{23}\text{Na}$  MAS and MQMAS NMR Chemical Shifts (ppm)**

	$\delta_{\text{MAS NMR}}$	$\delta_{\text{F2-MQMAS NMR}}$	$\delta_{\text{F1-MQMAS NMR}}$
vacuum	$-26.6$	$-26.8$	$-18.9$
oxygen (298 K)	$-24.2$	$-25.0$	$-16.9$
oxygen (250 K)	$-23.9$	$-24.4$	$-15.5$

temperatures. The interactions of the nuclear magnetic moments with the unpaired electron spin density decrease the transverse nuclear relaxation time ( $T_2$ ). The  $T_2$  relaxation time is inversely proportional to the peak width so that smaller  $T_2$ 's will produce broader peaks. We have not explored this effect quantitatively, but others have done so for  $^1\text{H}$  NMR.<sup>4</sup> Qualitatively, our results show the same trends.

Similar experiments have been run using  $^7\text{Li}$  MAS NMR to test the accessibility of lithium cations located in site III of zeolite X.<sup>1,3</sup> It has been found that at low temperatures there is a significant paramagnetic shift of the lithium resonance due to the presence of oxygen, much larger than the sodium site III resonance seen in our  $^{23}\text{Na}$  MAS NMR experiments. The difference in these paramagnetic shifts for lithium and sodium is related to the quadrupole moments of these two cations ( $^7\text{Li}$   $q = -4 \times 10^{-30}$  Q/m<sup>2</sup>;  $^{23}\text{Na}$   $q = 1 \times 10^{-29}$  Q/m<sup>2</sup>). The larger quadrupole moment for  $^{23}\text{Na}$  will lead to larger quadrupolar interactions and thus a larger quadrupolar shift of the sodium site III resonance over the lithium site III resonance. This upfield quadrupolar shift is in the opposite direction of the paramagnetic shift and therefore can lead to a smaller overall downfield shift for the sodium cations. In the following section we demonstrate using  $^{23}\text{Na}$  MQMAS NMR that in this particular sample the quadrupolar shift does indeed increase as the temperature decreases.

**$^{23}\text{Na}$  MQMAS NMR ( $B = 500$  MHz).** Figure 3 shows the 1D spectra of the F1 dimension from the 2D  $^{23}\text{Na}$  MQMAS NMR spectra (in these spectra, the signal from the glass insert was not removed). In the  $^{23}\text{Na}$  MAS NMR experiments it was found that the glass insert signal under all temperatures and regardless of adsorbed molecular oxygen did not change the peak position for the site III cations. Therefore, the peak positions from the 2D MQMAS NMR spectra are unaffected by the glass insert's sodium signal (Table 1.). The F2 dimension of the data represents the anisotropic chemical shifts; i.e., the peak positions in this dimension should be the same as those seen in the single pulse  $^{23}\text{Na}$  MAS NMR spectra (Figure 2). The dehydrated site III F2 resonance was located at  $-26.82$  ppm, which is nearly the same as in the MAS NMR (spectra not shown). The site III resonance for the oxygen-containing sample was located at  $-25.0$  and  $-24.4$  ppm for the room-temperature (298 K) and low-temperature (250 K) spectra, respectively. These peak positions are the same as those



**TABLE 2:  $^{23}\text{Na}$  MQMAS NMR Isotropic Chemical Shifts, Second-Order Quadrupolar Shifts, and Quadrupolar Coupling Constants**

	$\delta_{\text{iso}}$ (ppm)	$q$ (ppm)	QCC (MHz) $\eta = 0$	QCC (MHz) $\eta = 1$
vacuum	-21.8	-5.0	1.9	1.6
oxygen (298 K)	-19.9	-5.12	1.9	1.6
oxygen (250 K)	-18.8	-5.6	2.0	1.7

measured in the variable-temperature 1D MAS NMR spectra (within experimental error).

The F1 isotropic dimension spectra can be seen in Figure 3. The chemical shift for the resonances (Table 1) in this dimension will be effected by the chemical environment surrounding the sodium, the quadrupolar interactions and the paramagnetic shift interactions due to the presence of oxygen. Although the quadrupolar effects are still present in the F1 dimension, they are smaller than those found in the 1D  $^{23}\text{Na}$  MAS NMR spectra. The F1 dimension  $^{23}\text{Na}$  MQMAS NMR spectrum for the sample under vacuum is shown in Figure 3a. The site III resonance is located at -18.9 ppm. Upon the addition of oxygen, the room-temperature site III resonance is shifted downfield to -16.9 ppm (Figure 3b). At 250 K, this peak is shifted even further to -15.5 ppm (Figure 3c).

The low-temperature (MQMAS) paramagnetic shift for the oxygen-containing sample in the F1 dimension is larger than that observed in the  $^{23}\text{Na}$  MAS NMR spectra (0.3 ppm vs 1.4 ppm). This difference in the shifts is evidence that changes in quadrupolar effects take place during the variable-temperature NMR experiments. The MQMAS experiments decrease quadrupolar interactions, which will result in smaller upfield quadrupolar shifts of the resonance, and hence a larger overall downfield shift will be observed in the 1D F1 MQMAS spectrum.

The values for the isotropic chemical shift, second-order quadrupolar shift, and quadrupolar coupling constant can be seen in Table 2. The site III isotropic chemical shift for the sample under vacuum was found to be -21.8 ppm. Upon the addition of oxygen this resonance is shifted to -19.9 ppm at room temperature and to -18.8 ppm at 250 K. The observed paramagnetic isotropic chemical shift is less than that found in the MQMAS F1 dimension spectrum due to the fact that the isotropic chemical shift is still affected by quadrupolar interactions.

The second-order quadrupolar shift and quadrupolar coupling constant for the sample under vacuum and the oxygen-containing room-temperature sample were very similar in magnitude (see Table 2). Therefore, the presence of oxygen does not greatly affect the quadrupolar interactions and the observed shift seen in the room-temperature MAS NMR spectra (Figure 2) is mainly attributed to the paramagnetic effect of the oxygen. However, the oxygen-containing sample run at low temperatures produces a larger quadrupolar shift and QCC, indicating that for this site the temperature does affect the quadrupolar interactions. This larger upfield quadrupolar shift will result in a smaller observed downfield paramagnetic shift for the low-temperature oxygen sample in the  $^{23}\text{Na}$  MAS NMR spectra (Figure 2).

## Conclusions

$^{23}\text{Na}$  MAS NMR and  $^{23}\text{Na}$  MQMAS NMR spectroscopy were used to investigate the site III sodium cations in LiNaX. The

site sodium III cations experienced a paramagnetic shift of their NMR resonance due to the interaction of the cations with oxygen molecules. Contrary to the results found for  $^7\text{Li}$ ,<sup>1,3</sup> our results indicate that using adsorbed oxygen to discriminate between accessible and inaccessible sodium cations is difficult. This is because the sodium shifts are small and because changes in the QCC with temperature confound the interpretation of NMR spectra.

The isotropic chemical shifts, second-order quadrupolar shifts, and quadrupolar coupling constants were also calculated from  $^{23}\text{Na}$  MQMAS NMR. The quadrupolar shifts and QCC remained the same irrespective of the presence or absence of oxygen. Therefore, a significant downfield paramagnetic shift was observed in the MAS NMR spectra for the oxygen-containing sample. However, this upfield quadrupolar shift increased at lower temperatures such that a smaller overall downfield shift was observed in the low-temperature MAS NMR spectra.

**Acknowledgment.** We thank H. Eckert and the Institute of Physical Chemistry at the University of Münster for the use of their 500 MHz NMR spectrometer and Hubert Koller and Jerry Chan from the University of Münster for their help with the NMR experiments. We also thank C. Dybowski and the Department of Chemistry and Biochemistry at the University of Delaware for the use of their 300 MHz NMR spectrometer. We thank Matthias Feuerstein for useful discussions regarding  $^{23}\text{Na}$  MAS and MQMAS NMR. Funding was provided by the National Science Foundation through a CAREER (CTS-9733066) award to Raul F. Lobo and a National Science Foundation Travel Award (INT-9725941).

## References and Notes

- Feuerstein, M.; Lobo, R. F. *Chem. Commun.* **1998**, 16, 1647.
- Feuerstein, M.; Lobo, R. F. *Chem. Mater.* **1998**, 10, 2197.
- Plevert, J.; Menorval, L. C. d.; Renzo, F. D.; Fajula, F. *J. Phys. Chem. B* **1998**, 102, 3412.
- Liu, H.; Kao, H.-M.; Grey, C. P. *J. Phys. Chem. B* **1999**, 103, 4789.
- Zscherpel, D.; Brunner, E.; Koch, M. *Z. Phys. Chem.* **1995**, 190, 123.
- Bertini, I.; Luchinat, C. *NMR of Paramagnetic Molecules in Biological Systems*; Benjamin/Cummings Publishing Co., Inc.: Menlo Park, CA, 1986.
- Accardi, R. J.; Lobo, R. F. *Micropor. Mesopor. Mater.* **2000**, 40, 25.
- Harris, R. K. *Nuclear Magnetic Resonance Spectroscopy*; Pitman: London, 1983.
- Medek, A.; Marinelli, L.; Frydman, L. *Multiple-Quantum Magic-Angle Spinning NMR of Half-Integer Quadrupolar Nuclei*; Oxford University Press: Washington, DC, 1999.
- Frydman, L.; Harwood, J. S. *J. Am. Chem. Soc.* **1995**, 117, 5367.
- Medek, A.; Harwood, J. S.; Frydman, L. *J. Am. Chem. Soc.* **1995**, 117, 12779.
- Hunger, M.; Sarv, P.; Samoson, A. *Solid State Nucl. Magn. Reson.* **1997**, 9, 115.
- Sarv, P.; Wichterlova, B.; Cejka, J. *J. Phys. Chem. B* **1998**, 102, 1372.
- Engelhardt, G.; Kentgens, A. P. M.; Koller, H.; Samoson, A. *Solid State Nucl. Magn. Reson.* **1999**, 15, 171.
- Feuerstein, M.; Engelhardt, G.; McDaniel, P. L.; MacDougall, J. E.; Gaffney, T. R. *Micropor. Mesopor. Mater.* **1998**, 26, 27.
- Massiot, D.; Touzo, B.; Trumeau, D.; Coutures, J. P.; Virlet, J.; Florian, P.; Grandinetti, P. *J. Solid State Nucl. Magn. Reson.* **1996**, 6, 73.
- Breck, D. W. *Zeolite Molecular Sieves*; John Wiley & Sons: New York, 1974.
- Engelhardt, G.; Michel, D. *High-Resolution Solid-State NMR of Silicates and Zeolites*; John Wiley & Sons: Chichester, U.K., 1987.
- Feuerstein, M.; Hunger, M.; Engelhardt, G.; Amoureux, J. P. *Solid State Nucl. Magn. Reson.* **1996**, 7, 95.